Experimental feasibility of Electrochemical Infiltration of Laser Sintered Preforms

Abhishek Goel and David Bourell
Laboratory for Freeform Fabrication, The University of Texas at Austin
1 University Station, MC C2200
Austin, Texas 78712
USA
+512-471-3170 voice, +512-471-7681 fax
agoel@mail.utexas.edu, dbourell@mail.utexas.edu

Reviewed, accepted September 23, 2010

Abstract

This research deals with the experimental feasibility of room temperature infiltration of Selective Laser Sintered preforms with metals. The existing principles of electrochemical deposition techniques were adapted and modified for carrying out the infiltration at low temperatures. Electroless and electrolytic deposition processes were adapted and modified to carry out metal ion infiltration and deposition within interconnected pores. The electrolytic infiltration process was modified by inserting a conductive graphite cathode in the center to draw the positive nickel ions through the interconnected porous network and to deposit them on the pore walls. Forced diffusion method was also attempted by forcing the electrolyte through the preform at high pressures. One of the major benefits of electrochemical infiltration is low processing temperature. Low temperature reduces both energy consumption and associated carbon-footprint and also minimizes undesirable structural changes. Both conductive and non-conductive preforms may be electrochemically infiltrated, and MMCs produced by this method have potential for use in structural applications. This research is sponsored by the National Science Foundation, Grant CMMI-0926316.

Introduction

This work deals with electrochemical infiltration of parts fabricated using one of the most common powder processing additive processes, Selective Laser Sintering (SLS). Powder metallurgy and melt infiltration are the most common techniques for producing metallic matrix composites (MMCs). A common feature of these techniques is high processing temperature which is a major cause for high production costs, poor mechanical properties and high sustainability penalty. Electrochemical deposition is a technique which is most commonly used to deposit a thin film coating on various types of material substrates. In the following work the principles of electrochemical deposition are used to carry out electrochemical infiltration of metal ions into sintered preforms. One of the major advantages of electrochemical infiltration is the lower processing temperature, normally room temperature, which helps to avoid undesirable chemical and structural changes. When electrochemical techniques are applied to form MMCs, the working conditions become much more complicated. The electrolyte must transport to the interior porous structure through narrow channels and at the same time the by-products of reaction must be driven out of the preform. This work aims at facile, low-cost room-temperature infiltration of selective laser sintered preforms to create fully functional dense parts. Selective

laser sintering is a commercial, powder-based manufacturing process that produces parts with arbitrary shape based on a computer solid model. Fig. 1 shows a schematic of the process. Powder is spread as a thin layer approximately 125 microns thick. A computer-controlled laser scans the surface and melts together the powder, creating a thin cross section of the part. Alternatively, the powder may be mixed with a transient binder which melts under the scanning laser beam and is removed or converted in a post-processing step. This process is repeated thousands of times to create an entire part with virtually unlimited geometric complexity. Indirect SLS parts are typically 50-65 percent dense with virtually all porosity being open or connected. The average pore size is typically the order of the powder size, approximately 30-60 microns. In electrochemical deposition, this pore network is filled with an electrolytic liquid, and deposition of a solid phase is initiated internally. The time required to close a pore is short since only a pore radius (~15-30 microns) needs to be deposited for closure. The porosity was measured using pychnometry and is shown in Table 1. The theoretical density of silicon carbide is about 3.22g/cc.

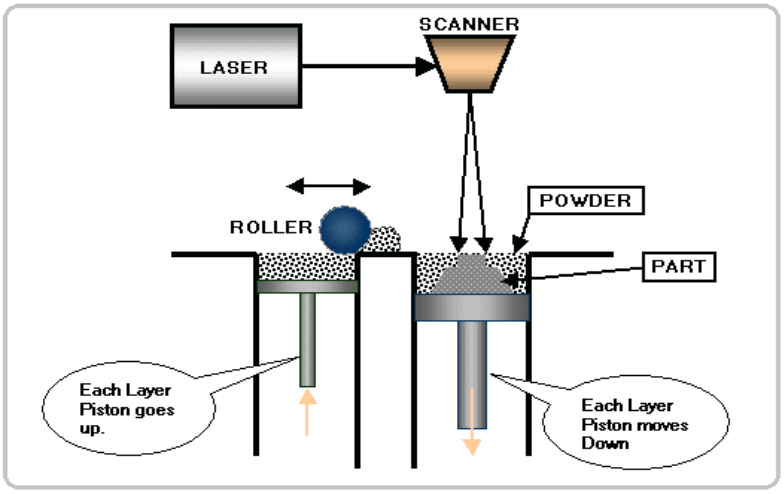

Figure 1. Schematic of Selective Laser Sintering

Table 1. Pychnometer Porosity Measurements of Silicon Carbide SLS Brown Parts

Mass (g)	Apparent Volume (cc)	Pychnometer Volume (cc)	Apparent density (g/cc)	Porosity (%)
37.07	25.87	12.27	1.43	52.57
35.95	25.56	12.32	1.41	51.68
32.85	23.79	11.63	1.38	51.11

By control of the deposition process spatially, the electrolytic liquid may be successfully ejected in front of the deposition. First, the non-metallic/metallic phase is mixed in powder form with an appropriate binder powder. The mixture is then SLSed to create a porous “green” part bound by the binder. After this the green part is converted to a “brown” part by heating to dissociate the binder. In this way organic ligaments or bridges between individual powder particles are replaced by a residue of equal or greater bond strength. The brown part is then infiltrated by dipping it in a bath containing a metallic salt as an electrolyte. Metal ions diffuse into the porous network of the brown preform where they combine with a counter electron flow

resulting in metallic deposition within the pore network [1-4]. Silicon carbide is an engineering ceramic for which the indirect SLS process has a great potential. This material is of interest where high-temperature strength and stability are required, and where wear and corrosion are issues. Some of its numerous applications include electronics processing wafer carriers and boats, kiln components and wear parts. However, silicon carbide objects, and non-metallics in general, are often difficult to manufacture due to their high melting temperatures (around 2700°C for SiC), poor sinterability, limited ductility and difficulty to machine. Selective laser sintering coupled with electrochemical infiltration offers a cost-effective and rapid manufacturing mechanism for metal-SiC composites. SiC is one of the potential candidates for high-temperature structural components. However, the most crucial aspect that limits the application of SiC-based ceramics is their brittleness. SiC is also quite difficult to densify because of the covalent nature of the Si-C bonding and a very low self-diffusion coefficient [5, 6]. Even liquid phase sintering is not able to provide highly dense SiC preforms, and the sintered preform is not free from pores. The average pore size in the solid phase sintered SiC preform has been seen to vary from 1μm to 100μm with an average pore size of 55μm. The porosity and strength varies according to Eq. (1):

$$E = E_0 \exp(-bP) \ , \ \sigma = \sigma_0 \exp(-bP) \tag{1}$$

E, σ = elastic modulus and strength of the porous structure, E_o, σ_o = elastic modulus and strength of the non-porous structure, P = porosity and b = constant dependent on pore shape. The deposition phenomena consist of several important facets such as the electrode-solution interface, kinetics and mechanism of the deposition process which includes surface and diffusion kinetics and nucleation and growth processes. The schematic of the process is shown in Fig. 2.
The mass of the deposit is w with the atomic weight of the metal M_w. The density of the deposited metal is ρ, V is the volume of the deposited metal in cc, A is the area of the deposit in cm^2 and T is the thickness in cm. The thickness of the deposit T is given by Eq. (2), where n = ionic charge and F = Faraday's constant.

$$T = \frac{w}{A\rho} = \left(\int Idt\right) \times \left(\frac{M_w}{nFA\rho}\right) \tag{2}$$

For the specific case of nickel deposition discussed here, the ionic radius of nickel (+2) ions are in the range 0.065-0.073 nm, its crystal radii vary in the range 0.079-0.087 nm, and standard electrode potential for nickel $E^0_{Ni^{2+}/Ni}$ = -0.25V [7]. The current densities usually range from 540/600 A/m^2 and the cathode efficiencies range from 93-97%. From Eq. (2), a 100 μm thick layer of nickel could be deposited on a 2 cm cube in 1 hr, which is reasonable for depositing metal ions on pore walls. Xu, et al. showed that the deposition distribution along the depth of the pore depends on the polarization factor ξ as the ratio of interfacial reaction rate to the diffusion rate of nickel inside the porous network [10, 11]. The polarization factor is a dimensionless parameter that depends of several critical parameters such as bulk concentration of Ni^{2+} ions, diffusion coefficient of Ni^{+2} ions, overpotential and exchange current density. Hence the major factor to be taken into account is the reduction of rate of deposition on the pore surface and higher diffusion rates inside the interconnected porous network. This can be achieved by controlling the polarization factor and inhibiting the deposition on the pore surface by using additives such as sodium allylsulfonate or coumarin. To increase the rate of diffusion of ions inside the porous network, external pressure may be applied to the electrolyte to force it through the preform. The pressure drop and the remaining porosity can be measured using Darcy's law.

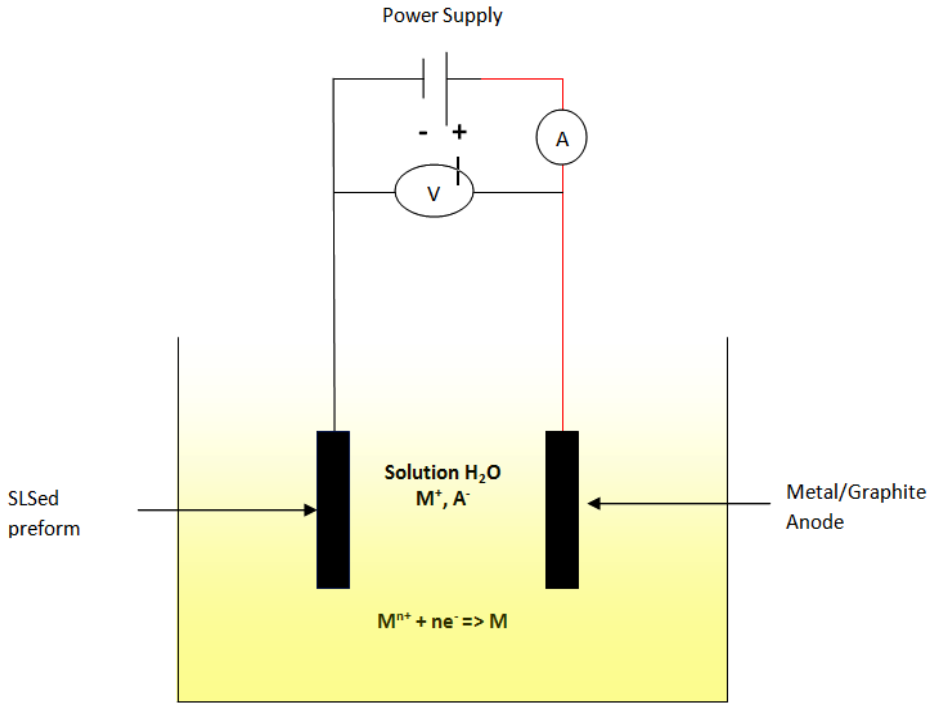

Figure 2. Schematic of Electrochemical Deposition Process

Experimental

Two types of infiltration experiments were carried out: electroless infiltration and electrolytic infiltration. In preparation for the infiltration experiments, 25 mm cubic samples were made using selective laser sintering. Initial experiments were carried out for the nickel-silicon carbide system. SiC preforms were made using SLS. 180 grit sizes commercially available SiC powder was mixed with the phenolic binder in the ratio 10:1 placed inside ball milling jars and allowed to mix for 6-8 hours at moderate speed. The mixed batch of powder was sifted to eliminate large sized particles. Prior to that, Differential Scanning Calorimetry (DSC) was carried out on neat phenolic powder to estimate its melting and curing temperatures. The plot obtained is shown in Fig. 3. The powder was loaded into the DTM-2000 Sinterstation, and the process was carried out at a part bed temperature of 115˚C and laser power of 20W, outlines laser power of 4W and slice thickness of about 75µm. Nitrogen process gas was used to maintain the inert atmosphere inside the machine chamber. After the green parts were obtained, these parts were burnt out in a high-temperature furnace at 180˚C/hr to 200˚C, then at 30˚C/hr to 500˚C and then at 300˚C/hr to 800˚C for brown part generation, then to 1400˚C at 250˚C/hr and finally to 1650˚C at 500˚C/hr. After this, the furnace was slowly cooled down and the final brown part was obtained.

Sample Preparation: The following steps were performed in the preparation of the sample for carrying out electrochemical infiltration. Firstly, the cubic SiC preform was cleaned in acetone for 15 minutes and then washed with distilled water. The preform was sensitized in 1L aqueous solution containing 10 grams of $SnCl_2$ and 40 ml of HCl, for 15 minutes and then again washed with distilled water. The preform was activated to open the surface pores by dipping it for 30 minutes in 1L aqueous solution 0.5 grams $PdCl_2$ and 30 ml HCl. The preform was washed and rinsed thoroughly for 10-15 minutes with distilled water [8, 9].

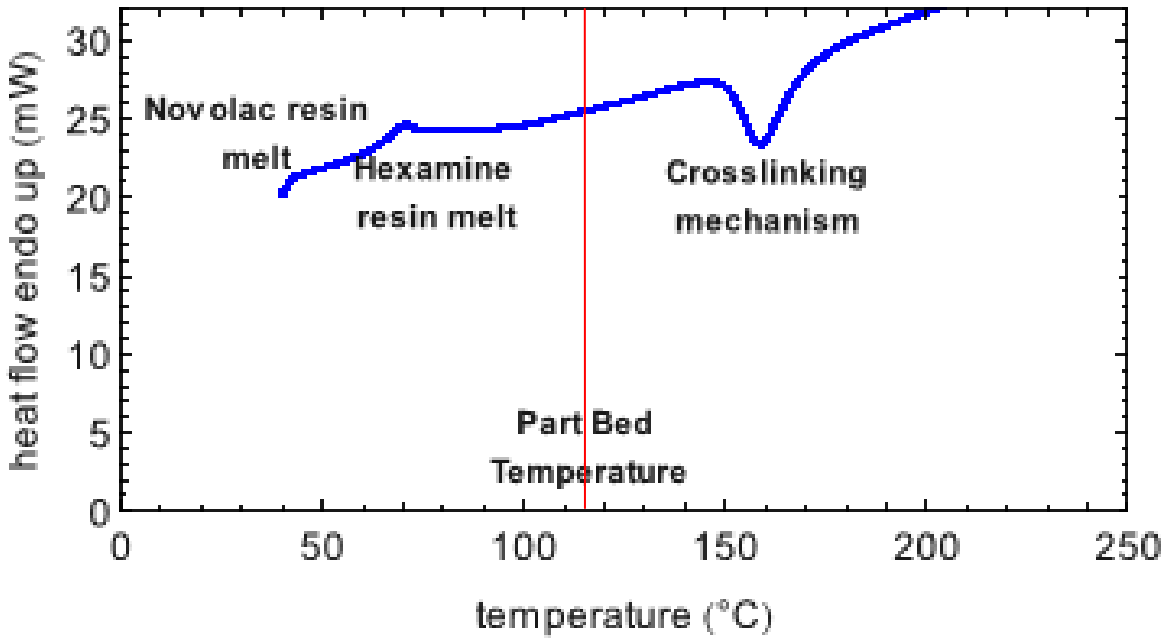

Figure 3. DSC of Phenolic Binder

Electroless Infiltration: The prepared sample was lowered into a bath containing 45 grams of nickel chloride (source), 8 grams of sodium hypophosphite (reducing agent), 100 grams sodium citrate (complexing agent) and 50 grams ammonium chloride (buffering agent) in 1L of distilled water at pH 9 and temperature of 80ºC. The bath was placed over a hot plate and was stirred using a magnetic stirrer. The process was carried out for 90 minutes [8].

Electrolytic Infiltration: The process was carried out by attaching a cathode terminal of the electrode to the sample and lowering it in a bath containing 225 grams nickel sulphate, 37.5 grams nickel chloride and 30 grams boric acid in 1L distilled water at pH 3.5. Bath temperature was maintained at 48ºC. The voltage applied between the electrodes was 2.5 V [9].

Modified Electrolytic Infiltration: The electrical conductivity of silicon carbide is very low, so a sufficient electronic charge concentration was not achieved uniformly throughout the sample. This inhibited the oxidation of metal ions to form a metallic deposit. To overcome this, preforms used as the cathode were modified by inserting a conductive graphite electrode at the center of the silicon carbide preform in two configurations as shown in Fig. 4.

Modified Electrolytic Infiltration of Graphite: The electrical conductivity of graphite is higher when compared to SiC. Thus similar modified infiltration technique as SiC was applied to the graphite preforms with copper rectangular cathode inserted at its center.

Forced Diffusion Method: The forced diffusion method was also tried out by forcing the electrolyte through the sample using a high pressure gear pump. The electroless forced diffusion method was tried out where no electrical connections were made to the sample. The schematic of the forced diffusion method is shown in Fig. 5(a) and the sample with the sample holder used is shown in Fig. 5(b).

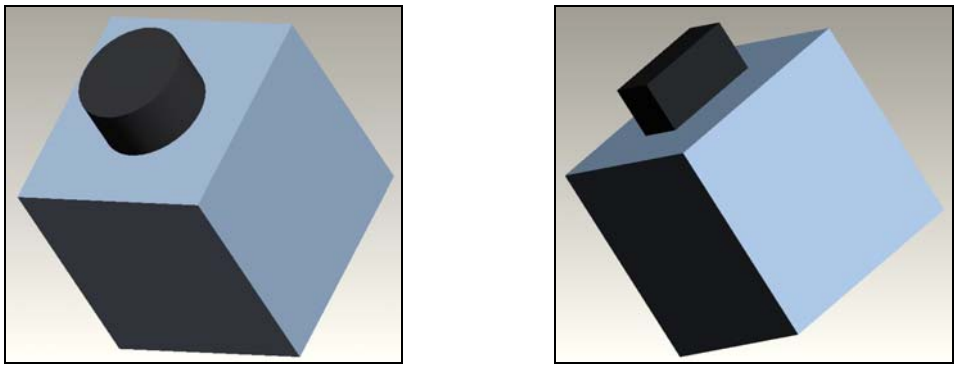

(a) (b)

Figure 4. (a) Modified Electrolytic Infiltration: Cylindrical Graphite Cathode (b) Modified Electrolytic Infiltration: Rectangular Plate Graphite Cathode

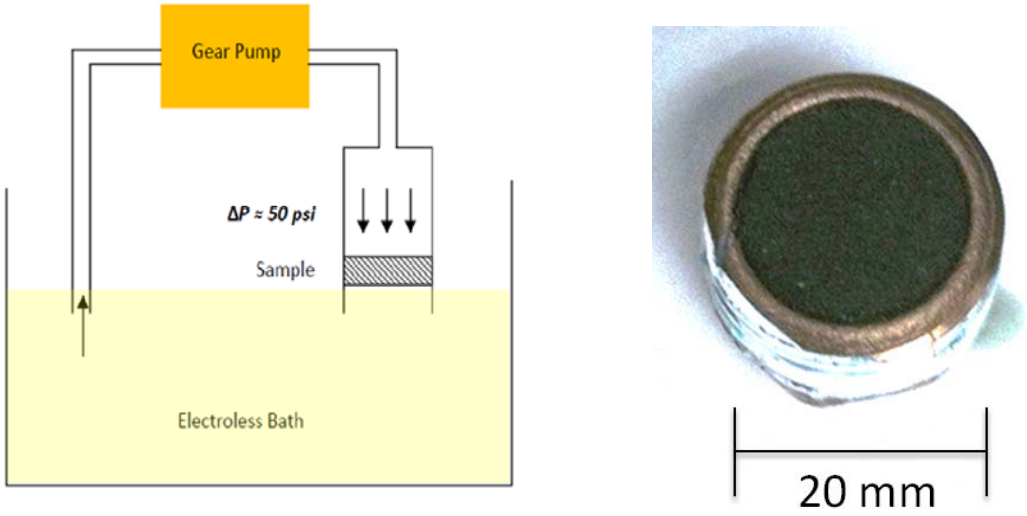

(a) (b)

Figure 5. (a) Schematic of forced diffusion process (b) Graphite Sample

The advantage of this modified process is that conductive graphite will attract most of the metal ions through the pores. After the surface of these graphite electrodes are completely saturated with the nickel metal deposits, and the reaction is still continued, the nickel metal will start depositing outwards on the pores and in this way a high part density can be achieved. After carrying out the infiltration experiments, the parts were kept inside a convection oven at 150ºC to dry them for SEM analysis and to remove trapped fluids and gases. EDS maps were obtained using a JEOL-JSM 5610 SEM equipped with an Oxford Instruments EDS system. The advantage of this modified process is postulated to be that conductive graphite will attract most of the metal ions through the pores. After the surface of these graphite electrodes are completely saturated with the nickel metal deposits, and the reaction is still continued, the nickel metal will start depositing outwards on the pores and in this way a high part density can be achieved. After carrying out the infiltration experiments, the parts were kept inside a convection oven at 150ºC to dry them for SEM analysis and to remove trapped fluids and gases.

Results and Discussion

The experiments were carried out for both electroless and electrolytic infiltration. The EDS maps showing the distribution of nickel is shown in Fig. 6. The maps were collected at a fractured cross section near the middle of a 1 inch cube infiltrated SiC preform. Fig. 6 shows the EDS maps collected using JEOL-JSM 5610 SEM with Oxford Instruments EDS system. The results are encouraging because Fig. 6 shows that it is possible to infiltrate porous preforms with metal ions using electrochemical techniques by overcoming the surface deposition barrier. The results provide a motivation to carry out other high diffusion rate processes to completely fill the pores and obtain high density functional parts. The EDS maps show that significant amounts of nickel were seen in the preforms without any external diffusion. If an external diffusive force is applied, then higher concentrations of nickel can be seen to occupy the pores. One issue is the removal of undesirable trapped gases and fluids from the bath which may occupy a large portion of the porous network. Fig. 7 shows the SEM images of the preform at a fractured cross-section, for the modified electrolytic infiltration – configuration b. It can be seen from these SEM images that modified electrolytic infiltration has been quite effective in depositing the metals in the pores of the SLSed silicon carbide preform. The forced diffusion method is not found to be as effective as compared to the modified electrolytic infiltration techniques. This might be due to very high pumping pressure of the electrolyte through the preform.

Electroless Infiltration

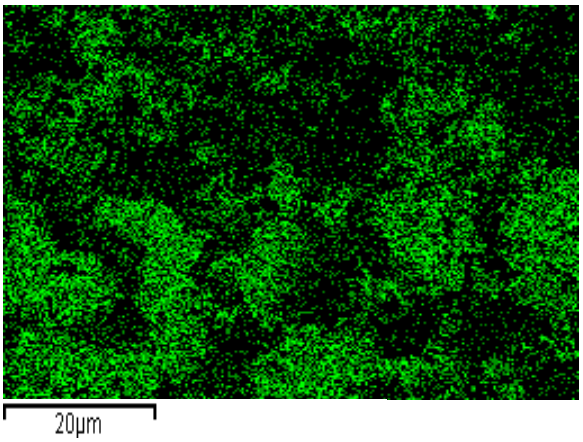

Electrolytic Infiltration

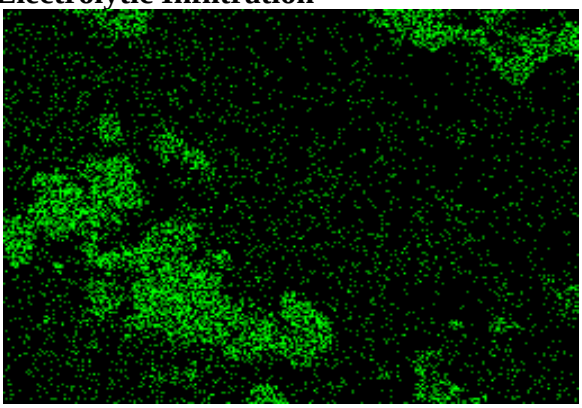

Modified Electrolytic Infiltration (a)

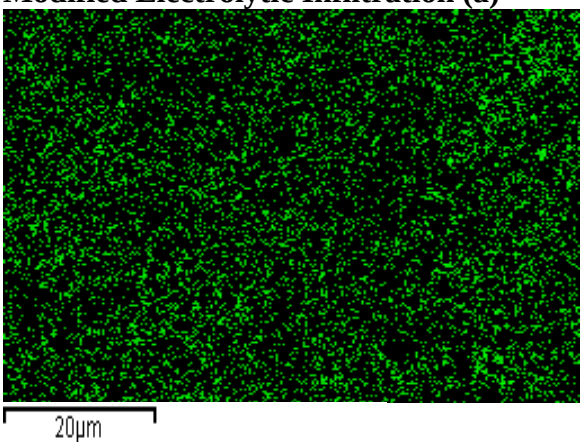

Modified Electrolytic Infiltration (b)

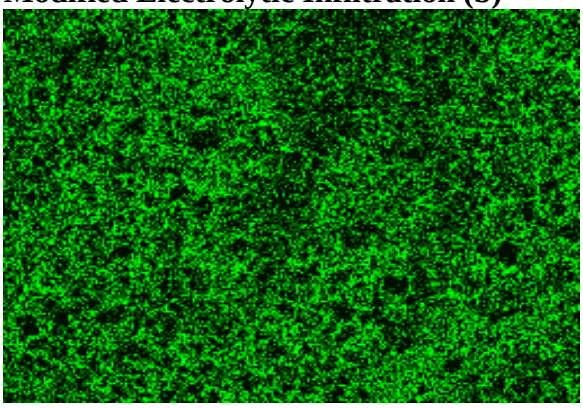

Forced Diffusion Method **Modified Electrolytic Infiltration Graphite**

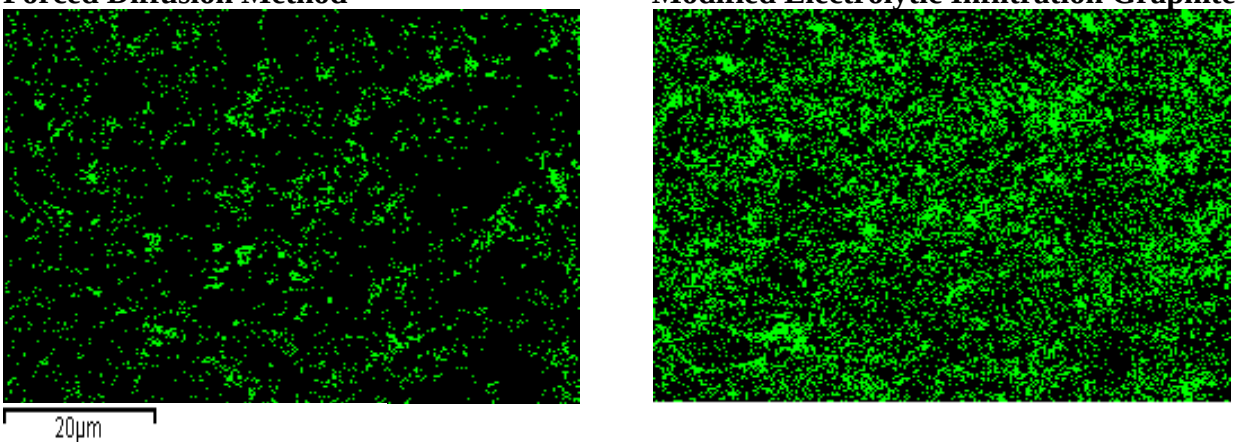

Figure 6. EDS maps showing relative distribution of silicon, carbon and nickel after infiltration

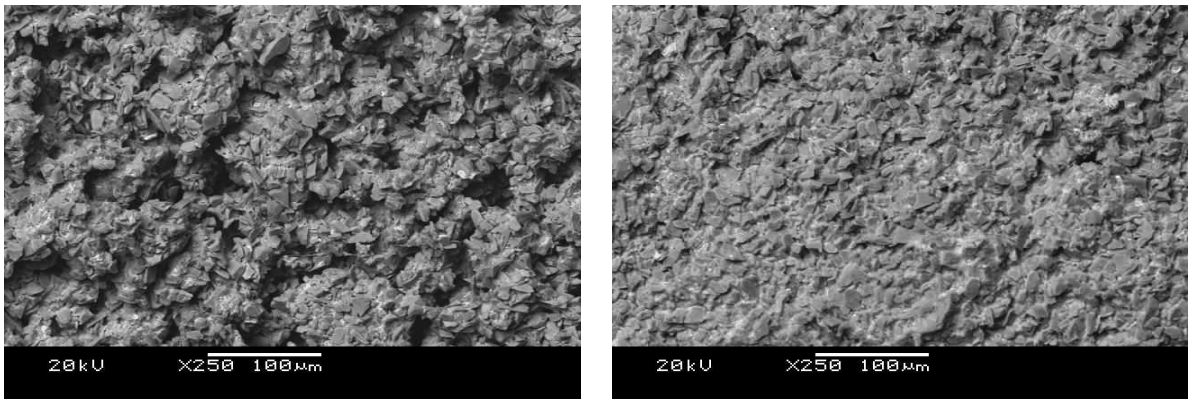

Figure 7. SEM images showing the fractured cross section (a) before (b) after the infiltration

Table 2 shows the weight percentage of nickel deposited in the pores inside the preform in each of the infiltration methods described above. It shows that modifying the process of electrochemical plating by inserting a conducting electrode at the center of the SLSed preform leads to an increase in the percentage of nickel deposited in the pores. Higher concentrations of nickel should be achieved by reducing the current density and applying external diffusion. The target composition of nickel to achieve 100% dense part is around 65-70% by weight.

Table 2. Weight % of Nickel obtained after carrying out each infiltration process

Process	Average % Nickel (by weight)
Electroless Infiltration	6.4
Electrolytic Infiltration	3.8
Modified Electrolytic Infiltration 1	9.8
Modified Electrolytic Infiltration 2	18.6
Modified Electrolytic Infiltration Graphite	16.6
Forced Diffusion Method	6.2

It can be seen from Table 2 that the weight percentage of nickel obtained in the preform after infiltration is better in case of configuration b as compared to configuration a. Similar is the case with the modified infiltration of graphite. This is because configuration b provided a larger surface area for the ions to be deposited and especially on one side of the electrode which was parallel and facing the anode. The rate of deposition was faster on this side compared to the other side. As a result, more amount of nickel was deposited on the walls of the pores. Hence, orientation of the two electrodes does matter in case of electrochemical deposition which can be easily resolved by using two anodes on either side of the cathodic preform. Fig. 8 shows the comparison chart for various infiltration methods and Table 3 shows the comparison between various infiltration processes in terms of energy consumption.

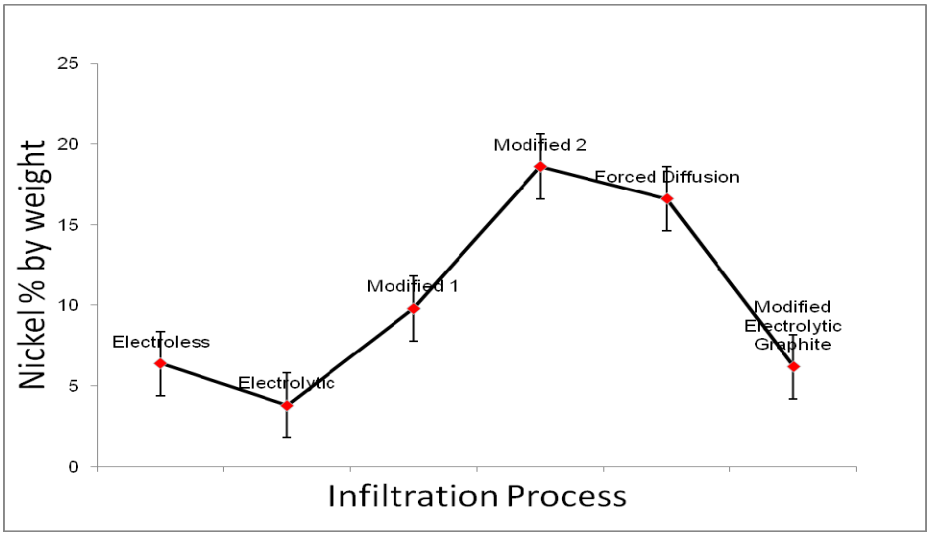

Figure 8. Plot showing the concentration of nickel for different infiltration methods

Table 3. Energy comparison for various kinds of infiltration process

Process	Estimated Power Consumption(kW)
Vacuum Melt Infiltration	18-24
Electrochemical Infiltration	0.7-0.9
Forced Electroless Infiltration	0.8-1.6
Chemical Vapor Infiltration*	6.8-10

One of the major challenges faced in the current situation relates to the depletion of desired ions into the small pores (where the solution is not assumed to be well-stirred). Initial experiments were carried out just to demonstrate and observe the feasibility of the concept. While the results show incomplete closure of the void network, they are nonetheless encouraging since a significant amount of nickel was deposited deep inside the pores network. It is anticipated that external diffusion techniques may well force the electrolyte in and out of the porous preform to improve the extent of deposition.

Conclusions and Future Work

Infiltration of SLS silicon carbide preforms with nickel led to encouraging results. The initial stages of work show that the electrochemical infiltration of SLS preforms with metals is highly feasible and has the potential to produce fully dense parts without any undesirable changes. Future work includes exploring other deposition techniques and comparison of those results to these. Ionic diffusion affects the infiltration process to a great extent and hence methods having enhanced diffusion rates such as pressurized diffusion of electrolyte into the preform need to be assessed. Other techniques include electrophoretic infiltration in which the charged ions move relative to the electrolyte, through the porous network under the action of applied field. Electroosmotic methods can also be tried where the electrolyte moves with respect to the stationary charged surface. Another important issue is identification of a method for driving the trapped gases and electrolyte out of the porous structure. Infiltration of freeform fabricated parts is a densification method shown to maintain dimensional stability of the part to a high degree and to enable freeform creation of functional parts.

References

1. H. B. Zhao et al, “Preparation of Palladium composite membranes by modified electroless plating procedure”, Journal of Membrane Science, vol. 142, pp. 147-157. 1998

2. M. Palaniappa, G. Veera Babu, K. Balasubramanian, “Electroless nickel-phosphorus plating on graphite powder”, Materials Science and Engineering, vol. 471, pp. 165-168, 2007

3. L. F. Chen, X. T. Luo, Q. L. Wu, Electrochemical preparation of fiber reinforced metallic matrix composites, Journal of Materials Science Letters 2003, 23, pp. 379-381

4. J. Duck et al, Infiltration as post processing of laser sintered metal parts, Powder Technology, 2004, 145, pp. 62-68

5. A. L. Burykina, L. V. Strashinskaya, T. M. Evmshok, “Investigation of the interaction of silicon carbide with refractory metals and oxides”, vol. 4 (3), pp. 301-305, 1968

6. K Motzfeld, “Silicon carbide: synthesis, structure and properties”, Proceedings of the International Conference on Engineering Ceramics, edited by M Haviar, Reprint (Bratislava, 1993) pp. 7–42, 1992

7. Short Communications, “The ionic radius of nickel”, Mineralogical Magazine, vol. 37, pp 286, 1969

8. F. Kretz et al, “The electroless deposition of Nickel on SiC particles for aluminum matrix composites”, Surface and Coatings Technology, vol. 180-181, pp. 575-579, 2004

9. T. J. Lee et al, “Synthesis of a nanophase, whisker-reinforced, ceramic/metal composite by electrochemical infiltration”, Journal of Materials Science, vol. 31, pp. 6555-6563, 1996